Biochimica et Biophysica Acta 1837 (2014) 1435–1446

Contents lists available at ScienceDirect

Biochimica et Biophysica Acta

journal homepage: www.elsevier.com/locate/bbabio

The importance of the hydrophilic region of PsbL for the plastoquinone electron acceptor complex of Photosystem II☆

Hao Luo [a,1], Simon A. Jackson [a], Robert D. Fagerlund [a,2], Tina C. Summerfield [b], Julian J. Eaton-Rye [a,*]

[a] Department of Biochemistry, University of Otago, P.O. Box 56, Dunedin 9054, New Zealand
[b] Department of Botany, University of Otago, P.O. Box 56, Dunedin 9054, New Zealand

ARTICLE INFO

Article history:
Received 7 January 2014
Received in revised form 12 February 2014
Accepted 15 February 2014
Available online 24 February 2014

Keywords:
Electron transfer
Herbicide binding
Photosystem II
PsbL
Q_B
Synechocystis sp. PCC 6803

ABSTRACT

The PsbL protein is a 4.5 kDa subunit at the monomer–monomer interface of Photosystem II (PS II) consisting of a single membrane-spanning domain and a hydrophilic stretch of ~15 residues facing the cytosolic (or stromal) side of the photosystem. Deletion of conserved residues in the N-terminal region has been used to investigate the importance of this hydrophilic extension. Using *Synechocystis* sp. PCC 6803, three deletion strains: Δ(N6–N8), Δ(P11–V12) and Δ(E13–N15), have been created. The Δ(N6–N8) and Δ(P11–V12) strains remained photoautotrophic but were more susceptible to photodamage than the wild type; however, the Δ(E13–N15) cells had the most severe phenotype. The Δ(E13–N15) mutant showed decreased photoautotrophic growth, a reduced number of PS II centers, impaired oxygen evolution in the presence of PS II-specific electron acceptors, and was highly susceptible to photodamage. The decay kinetics of chlorophyll *a* variable fluorescence after a single turnover saturating flash and the sensitivity to low concentrations of PS II-directed herbicides in the Δ(E13–N15) strain indicate that the binding of plastoquinone to the Q_B-binding site had been altered such that the affinity of Q_B is reduced. In addition, the PS II-specific electron acceptor 2,5-dimethyl-*p*-benzoquinone was found to inhibit electron transfer through the quinone-acceptor complex of the Δ(E13–N15) strain. The PsbL Y20A mutant was also investigated and it exhibited increased susceptibility to photodamage and increased herbicide sensitivity. Our data suggest that the N-terminal hydrophilic region of PsbL influences forward electron transfer from Q_A through indirect interactions with the D–E loop of the D1 reaction center protein. Our results further indicate that disruption of interactions between the N-terminal region of PsbL and other PS II subunits or lipids destabilizes PS II dimer formation. This article is part of a Special Issue entitled: Photosynthesis Research for Sustainability: Keys to Produce Clean Energy.

© 2014 Elsevier B.V. All rights reserved.

1. Introduction

Photosystem II (PS II) is a multi-subunit complex embedded in the thylakoid membrane of cyanobacteria, algae and plants where it catalyzes the oxidation of water and photoreduction of plastoquinone [1,2]. The structure of PS II from the thermophilic cyanobacteria *Thermosynechococcus elongatus* and *Thermosynechococcus vulcanus* has been obtained by X-ray crystallography [3–5]. These studies have shown PS II to be dimeric, with each monomer containing the chlorophyll *a*-binding core antenna proteins CP43 and CP47 together with the D1/D2 reaction center subunits and at least 16 additional polypeptides and 70 cofactors [3–6]. The complexity of PS II is in contrast to the purple bacterial reaction center, which contains 4 subunits and 14 cofactors [7], despite structural and functional similarities in the core reaction centers of these related photosystems [8–10].

The structural complexity of the PS II supercomplex is in part attributed to the presence of low-molecular-weight (LMW) transmembrane polypeptides [11–13]. Thirteen LMW subunits have been identified on the periphery of each PS II monomer [3–6]. Gene inactivation studies suggest that the absence of these subunits frequently results in mutants

Abbreviations: BN-PAGE, Blue-native polyacrylamide gel electrophoresis; DCMU, 3-(3,4-Dichlorophenyl)-1,1-dimethylurea; DM, n-Dodecyl β-D-maltoside; DCBQ, 2,6-Dichlorobenzoquinone; DCPIP, 2,6-Dichlorophenolindophenol; DMBQ, 2,5-Dimethyl-*p*-benzoquinone; HEPES, 4-(2-Hydroxyethyl)-1-piperazineethanesulfonic acid; I_{50}, Concentration of inhibitor to reduce activity by 50%; Kb, Kilobase; K_D, Apparent dissociation constant; kDa, Kilodalton; OD, Optical density; OEC, Oxygen-evolving complex; PCC, Pasteur Culture Collection; PCR, Polymerase chain reaction; PQ, Plastoquinone; PS II, Photosystem II; Q_A, Primary quinone electron acceptor of Photosystem II; Q_B, Secondary quinone electron acceptor of Photosystem II; S states, Oxidation states of the manganese–calcium cluster of the oxygen-evolving complex of Photosystem II; TES, 2-[Tris(hydroxymethyl)methyl]amino-1-ethanesulfonic acid; Tris, Tris(hydroxymethyl) aminomethane

☆ This article is part of a Special Issue entitled: Photosynthesis Research for Sustainability: Keys to Produce Clean Energy.

* Corresponding author. Tel.: +64 3 479 7865; fax: +64 3 479 7866.
E-mail address: julian.eaton-rye@otago.ac.nz (J.J. Eaton-Rye).
[1] Current address: Novo Nordisk Foundation for Biosustainability, Technical University of Denmark, Kogle Alle 4, Hørsholm 2970, Denmark.
[2] Current address: Department of Biochemistry and Molecular Biology, The Pennsylvania State University, University Park, PA 16802, USA.

http://dx.doi.org/10.1016/j.bbabio.2014.02.015
0005-2728/© 2014 Elsevier B.V. All rights reserved.

with impaired photoautotrophic growth or PS II assembly [14–17]. In addition, although LMW subunits do not appear to directly participate in linear photosynthetic electron transport, several subunits have been shown to regulate electron flow within PS II [18–21].

The PsbL protein is one of three LMW polypeptides (the others are PsbM and PsbT) located at the monomer–monomer interface of the cyanobacterial PS II crystal structure [3–6]. This highly conserved ~4.5 kDa subunit consists of a single transmembrane helix and a cytosol-exposed N-terminal region. Inactivation of *psbL* in the cyanobacterium *Synechocystis* sp. PCC 6803 (hereafter *Synechocystis* 6803) severely retarded photoautotrophic growth [21,22].

It has been suggested that the C-terminus of PsbL is required for the oxidation of the redox active tyrosine Y_Z on the D1 protein by the oxidized primary donor of PS II, $P680^+$, as determined by electron paramagnetic resonance spectroscopy using PsbL-reconstituted PS II complexes from spinach [23]. However, in the cyanobacterial PS II structure PsbL is not in the vicinity of Y_Z or the adjacent oxygen-evolving complex (OEC). We investigated the role of the PsbL C-terminus in *Synechocystis* 6803 and found that the last four C-terminal residues were required for attachment of PsbL to the CP43-less PS II assembly intermediate complex. The failure of PsbL to dock to the CP43-less PS II complex in our mutant blocked the assembly of functional oxygen-evolving photosystems [24]. We also demonstrated that mutations targeting other conserved residues of the PsbL transmembrane domain resulted in increased susceptibility to photodamage.

Among the LMW subunits of PS II, PsbL is unique in having its N-terminal region exposed to the cytosolic side of the membrane. To extend our understanding of the role of PsbL in PS II, this hydrophilic stretch of residues has been investigated by the introduction of short deletions using site-directed mutagenesis in *Synechocystis* 6803.

2. Materials and methods

2.1. Synechocystis 6803 growth conditions

The glucose tolerant strain of *Synechocystis* 6803 [25] was grown in BG-11 media under constant illumination at ~30 μmol photons m^{-2} s^{-1}. Cultures were maintained on solid BG-11 plates in the presence of 5 mM glucose, 20 μM atrazine, 10 mM TES-NaOH (pH 8.2), 0.3% sodium thiosulfate and appropriate antibiotics [26]. The liquid cultures were grown mixotrophically in the presence of 5 mM glucose and appropriate antibiotics. In both solid and liquid media, the antibiotics used were chloramphenicol at 15 μg mL^{-1} and kanamycin at 25 μg mL^{-1}.

2.2. Generation of the PsbL mutant strains

The mutant strains were created using an oligonucleotide-directed PsbL mutagenesis system [24]. The Δ(N6–N8), Δ(P11–V12) and Δ(E13–N15) strains were made using oligonucleotides: 5′-ATGG ACAGAAATTCA//CGCCAACCGGTGGAA-3′, 5′-AACCCAAACCGCCAA// GAATTGAACCGCACT-3′ and 5′-AACCGCCAACCGGTG//CGCACTTCTTTA TAC-3′, respectively, where the two backslashes indicate the position of the deletion.

2.3. Measurement of photosynthetic activity

Photosynthetic activity was measured either by oxygen evolution in whole cells or by monitoring the reduction of 2,6-dichlorophenolindophenol (DCPIP) in isolated thylakoid membranes. Oxygen evolution in whole cells was performed according to [24]. For whole chain oxygen evolution measurements 15 mM sodium bicarbonate was used.

Isolation of thylakoid membranes from *Synechocystis* 6803 cells was performed according to [24]. Thylakoid membranes corresponding to 10 μg mL^{-1} of chlorophyll *a* were resuspended in the assay buffer (50 mM Tricine–NaOH (pH 7.5), 600 mM sucrose, 30 mM $CaCl_2$ and 1 M betaine) containing 100 μM DCPIP. The light-induced reduction of DCPIP was monitored spectrophotometrically at 590 nm using a Cary 118 UV–vis spectrophotometer (Varian, Palo Alto, CA, USA) and the sample was illuminated at room temperature with red light provided by a FLS2 light source (Hansatech, King's Lynn, UK) passed through a Melles Griot RG 665 optical filter. The photomultiplier was protected with a Melles Griot BG 38 filter.

2.4. PS II assembly

The relative level of assembled PS II reaction centers was estimated on a chlorophyll basis by employing a [^{14}C]-atrazine herbicide-binding assay [27,28]. Assembly of the PS II native complexes was visualized using blue native-polyacrylamide gel electrophoresis (BN-PAGE) followed by western blot analysis as described in [24]. The estimation of the level of PsbL expressed in the specific mutants was also determined with a PsbL-specific antibody as described in [24].

2.5. Variable chlorophyll a fluorescence measurements

Cells in liquid culture were harvested at an $OD_{730\ nm}$ of 1.0–1.2 (Jasco V-550 UV/vis spectrophotometer; Jasco International) by centrifugation at 2760 *g* for 10 min at room temperature and washed twice in buffered BG-11 containing 25 mM HEPES–NaOH (pH 7.5). Cells were resuspended at a chlorophyll *a* concentration of 10 μg mL^{-1} and incubated for 60 min under the standard growth conditions described above with constant shaking at 120 rpm. Prior to each measurement, cells were diluted 1:3 with fresh BG-11 (pH 7.5) media and incubated in the dark for 4 min at room temperature.

Variable chlorophyll *a* fluorescence measurements were performed using a double modulation fluorometer (PS I instruments, Brno, Czech Republic). Chlorophyll *a* fluorescence induction was measured over a period of 5 s under a continuous blue actinic light (455 nm) at 2800 μmol photons m^{-2} s^{-1}. Decay of the variable chlorophyll *a* fluorescence was measured in the 50 μs to 60 s time range after a 30 μs saturating single turnover flash (455 nm). Component analysis of the fluorescence relaxation kinetics attributed to forward and back electron transfer was performed according to [29]. When added, 3-(3,4-dichlorophenyl)-1,1-dimethylurea (DCMU) or diuron was at a final concentration of 40 μM and 2,5-dimethyl-*p*-benzoquinone (DMBQ) was at 200 μM.

2.6. Photodamage and recovery measurements

To assess the sensitivity of different mutants to photodamage, cells at 10 μg mL^{-1} were subjected to high intensity white light at 2000 μmol photons m^{-2} s^{-1} provided by a Kodak Ektalite 1000 slide projector for up to 45 min, followed by recovery under 30 μmol photons m^{-2} s^{-1} light provided by 250 W metal halide lamps [24]. When utilized, kanamycin (50 μg mL^{-1}) was added 10 min prior to starting the assay to prevent protein synthesis.

3. Results

3.1. Conserved residues in the N-terminus of PsbL

The PsbL N-termini of 34 cyanobacterial strains varied in length from 13 to 17 amino acids; the shortest were from *Gloeobacter violaceus* and *T. elongatus* and the longest from *Trichodesmium erythraeum* (Supplementary Fig. S1). In the majority of the cyanobacteria, including *Synechocystis* 6803, the hydrophilic region at the N-terminus contained 15 amino acids; however, even among these strains the first five amino acids were not conserved. Only four residues were conserved in all the cyanobacterial strains examined, and these were: Pro-7, Glu-13, Leu-14 and Asn-15 (numbers are based on the *Synechocystis* 6803 sequence). The Asn-6 and Asn-8 residues differed only in the PsbL

protein of *G. violaceus* which had Asp-6 and Lys-8. The Pro-11 was conserved in 33 out of 34 cyanobacterial strains (altered to Ser in *Prochlorococcus marinus* SS120) and the Val-12 residue was altered in three strains (Gly in *G. violaceus* and Ala in *Prochlorococcus marinus* MIT9313 and *P. marinus* MIT9303). Amino acids at positions 9 and 10 were less conserved (Supplementary Fig. S1). Based on these sequence comparisons deletion strains were constructed to target the more conserved amino acids in the N-terminal hydrophilic region (Fig. 1).

3.2. Characterization of PsbL N-terminal mutant strains

A mutagenesis system described in [24] was used to generate the amino acid deletions in PsbL in *Synechocystis* 6803. Three deletion mutants targeting the conserved residues within the PsbL N-terminus were created: Δ(N6–N8), Δ(P11–V12) and Δ(E13–N15), where this nomenclature indicates deletions from Asn-6 to Asn-8, Pro-11 to Val-12, and Glu-13 to Asn-15, respectively (Fig. 1). Complete segregation of the introduced mutations was confirmed by PCR and the presence of the mutated protein was confirmed by western blotting with an antibody to PsbL (Fig. 2A). The control strain contained the antibiotic-resistance marker downstream of *psbL* as in the mutants but apart from antibiotic resistance its phenotype could not be distinguished from the wild type [24]. All mutant strains grew photoautotrophically although growth of the Δ(E13–N15) strain was severely impaired with a doubling time > 50 h, whereas the Δ(N6–N8) and Δ(P11–V12) strains had growth rates that resembled those of the wild type and the control strain (Fig. 2B).

Whole chain oxygen evolution rates in the absence of exogenous electron acceptors were similar for the three mutants and the wild type under saturating actinic light (Fig. 2C). A number of PS II mutant strains in *Synechocystis* 6803 have been observed to retain the wild-type levels of oxygen evolution when the number of PS II centers is diminished (e.g., [30,31]). In addition, a lack of correlation between growth rates and oxygen evolution rates supported by artificial electron acceptors has been reported (e.g., [32,33]). Accordingly, the impact of the PsbL deletions on the number of assembled PS II centers was estimated using a herbicide-binding assay employing different concentrations of radiolabeled atrazine (Fig. 2D). The Δ(N6–N8) and Δ(P11–V12) strains had chlorophyll *a* to PS II ratios similar to the wild type (~450–630 chlorophyll/PS II); however, the Δ(E13–N15) mutant had a chlorophyll/PS II ratio of 1560 suggesting an approximately three-fold reduction of PS II centers in this strain.

Since the Δ(N6–N8) strain was photoautotrophic, evolved oxygen at a similar rate to the other strains and assembled photosystems with a chlorophyll/PS II ratio similar to the wild type, the absence of a signal in the western blot of this mutant was assumed to be due to the deletion resulting in a structural change in the epitope recognized by the antibody (Fig. 2A–D).

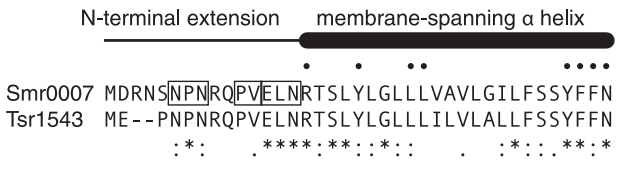

Fig. 1. PsbL protein sequence and structure. PsbL amino acid sequence of *Synechocystis* sp. PCC 6803 (Smr0007) and *Thermosynechococcus elongatus* BP-1 (Tsr1543). The boxes on the Smr007 sequence contain residues deleted in this study. The consensus symbols shown below the two sequences were annotated based on the alignment of 34 cyanobacterial PsbL protein sequences (Supplementary Fig. S1): fully conserved residues are marked with (*), highly conserved residues with conservative substitutions (:) and highly conserved residues with non-conservative substitutions (.). The thick solid black line above the alignment represents the α-helical membrane-spanning domain and the thin line represents an extended N-terminal region on the cytosolic side of the membrane. The C-terminus of PsbL does not protrude into the lumen. Residues in the C-terminus indicated with a black circle have been previously mutated [24].

3.3. Deletions in the PsbL N-terminal region destabilize the assembly of the PS II dimer

The reduced photoautotrophic growth and PS II assembly of the Δ(E13–N15) strain indicated that the hydrophilic N-terminus of PsbL may be important for maintaining optimal photosynthetic performance. As PsbL is at the dimer interface we investigated whether changes to PS II in the PsbL mutants include altered dimer formation. To assess PS II assembly, BN-PAGE followed by immunodetection using D1-specific and CP43-specific antibodies was used to determine the relative abundance of PS II dimers, monomers and other assembly intermediates. The abundance of the PS II native complexes in the Δ(N6–N8) strain was similar to the wild type (Fig. 3). In contrast, for the Δ(P11–V12) and Δ(E13–N15) strains, accumulation of PS II dimers was reduced and levels of the CP43-less monomer were elevated in these cells (Fig. 3). In this experiment a *psbA* deletion strain (described in [34]), lacking all three copies of the *psbA* gene encoding the D1 protein, was included as a control and no assembled centers were detected in this mutant.

3.4. PsbL deletion strains exhibit increased susceptibility to photodamage

To further investigate the impaired photoautotrophic growth in the Δ(E13–N15) mutant we next determined the susceptibility of our mutant strains towards photodamage. Following exposure to high-light stress PS II activity was measured using PS II-specific electron acceptors (membrane permeable DMBQ in the presence of the non-permeable oxidant $K_3Fe(CN)_6$). The Δ(E13–N15) cells were more susceptible to photodamage than the wild type with a rapid ~90% loss of the initial oxygen-evolving activity after 15 min of exposure at 2000 μmol photons m^{-2} s^{-1} and this reduced rate was maintained until the end of the high-light-treatment period (Fig. 4A). In contrast the wild type appeared to acclimate to the high-light treatment, with only a small decline in activity followed by restoration to initial levels. The other two mutant strains, Δ(N6–N8) and Δ(P11–V12), were susceptible to high light with oxygen evolution reduced by ~50% and ~70%, respectively (Fig. 4A). Upon transferring to low-light conditions (30 μmol photons m^{-2} s^{-1}) all three mutants were able to recover within 15 min. Indeed, all strains except the Δ(E13–N15) mutant exhibited oxygen evolution rates that exceeded their initial pre-treatment activity and maintained these elevated levels throughout the remainder of the low-light recovery period.

Previously a PsbL mutant (Y20A) was shown to be susceptible to photodamage in the presence of DMBQ and $K_3Fe(CN)_6$ to a similar extent to Δ(E13–N15) cells [24]. The Tyr-20 residue is located near the N-terminal beginning of PsbL's membrane-spanning domain and is highly conserved (Fig. 1). This residue differed in only 2 out of 34 cyanobacterial strains, *Synechococcus elongatus* sp. PCC 7942 and *Acaryochloris marina* MBIC11017, which had the conservative substitution of Phe at this position (Supplementary Fig. S1). Although the extent of photodamage between the Δ(E13–N15) and Y20A cells is similar the kinetics of inactivation in the Y20A were slower. While the Δ(E13–N15) cells are inactivated with a half-time of <15 min when exposed to high light, the Y20A cells exhibited a half-time of ~15 min and took ~45 min to be ~90% inhibited [24]. Nevertheless the recovery of both strains observed upon return to low light was similar.

As the photodamage phenotypes of the Δ(E13–N15) and Y20A strains were similar in the presence of PS II-specific acceptors we investigated the susceptibility of PS II to photodamage in both strains under conditions where whole chain electron transport was active. In contrast to the situation when oxygen evolution was supported by PS II-specific electron acceptors, whole chain electron transport in the presence of 15 mM bicarbonate was not susceptible to photodamage in the wild-type and Y20A cells and only a limited decline in oxygen evolution was observed in the Δ(E13–N15) mutant (Fig. 4B). Upon transferring

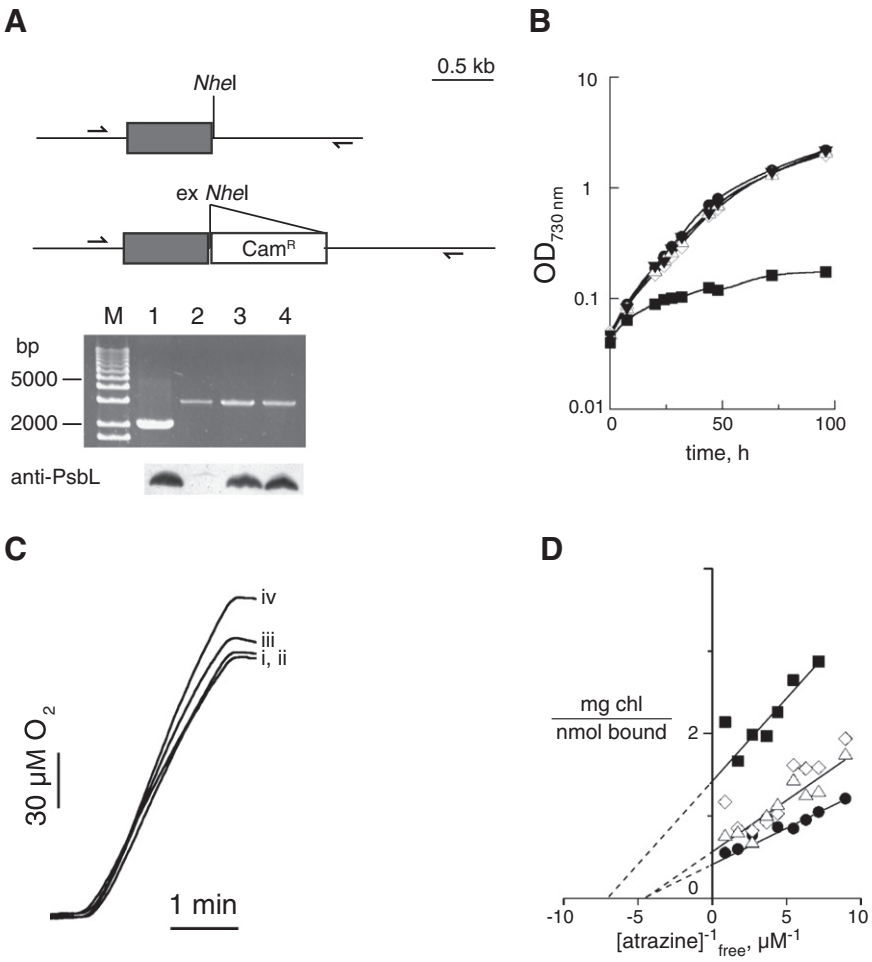

Fig. 2. Construction and characterization of PsbL mutants. (A) Top panel: Genomic maps showing the *psbEFLJ* operon (black box) and position of the chloramphenicol-resistance cassette (Cam^R) used to select for successful transformation of mutants into *Synechocystis* sp. PCC 6803. Arrows indicate the position of primers. Bottom panel: Segregation of the mutant strains checked by PCR and western blot. Molecular DNA marker, 1 kb Plus (Invitrogen, Carlsbad, CA, USA) (M), wild type (1), Δ(N6–N8) (2), Δ(P11–V12) (3), and Δ(E13–N15) (4). (B) Photoautotrophic growth of wild type (closed circles), control (closed inverted triangles), Δ(N6–N8) (open diamonds), Δ(P11–V12) (open triangles) and Δ(E13–N15) (closed squares) in BG-11 media as measured by the optical density at 730 nm. (C) Oxygen evolution traces of wild type (i), Δ(N6–N8) (ii), Δ(P11–V12) (iii), and Δ(E13–N15) (iv) in the absence of electron acceptors. (D) Double-reciprocal plots of [^{14}C]atrazine binding in these strains. The chlorophyll/PS II ratio of wild type (closed circles) was 446; Δ(N6–N8) (open diamonds) and Δ(P11–V12) (open triangles) was 626; and Δ(E13–N15) (closed squares) was 1562. The atrazine dissociation constant of wild type, Δ(P11–V12) and Δ(E13–N15) was ~250 nM and Δ(E13–N15) was 140 nM.

the cells back to low light, the wild-type cells increased their rate by ~25% above their initial rate at the beginning of the experiment and both mutants exhibited a similar increase.

To investigate the possibility that bicarbonate protects cyanobacterial cells from photodamage, PS II activity in whole cells was determined under photodamaging conditions in the presence of kanamycin. Fig. 4C

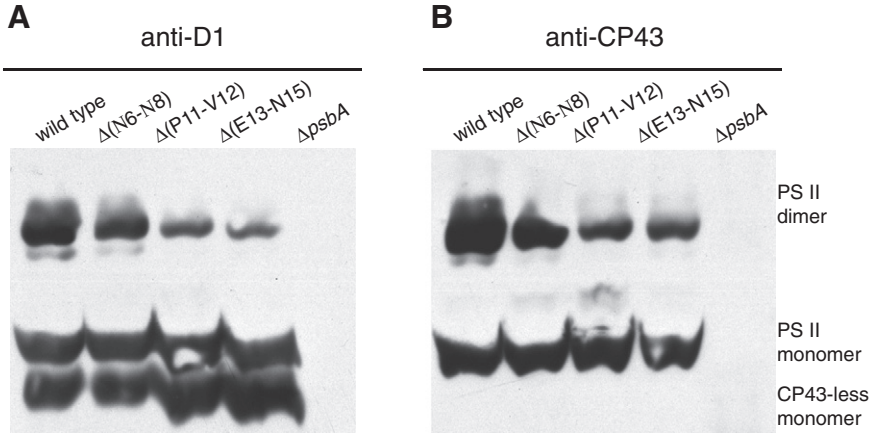

Fig. 3. Composition of PS II native complexes in the PsbL hydrophilic domain deletion mutants of *Synechocystis* sp. PCC 6803 shown by BN-PAGE. Native PS II complexes from thylakoid membranes were immunodetected using D1 (A) and CP43 (B) antibodies following separation by BN-PAGE.

demonstrates that when protein synthesis is blocked all strains were sensitive to high light and displayed a linear reduction in oxygen evolution. The oxygen-evolving capacity of the wild-type cells was reduced by ~40% at the end of the high-light exposure, and that of Y20A and Δ(E13–N15) cells by 50% and 85%, respectively. The oxygen-evolving rates in mutant cells did not recover upon removal of the light stress while kanamycin was present, indicating the requirement for de novo protein synthesis. Interestingly, the wild-type cells showed a partial recovery suggesting the existence of limited protein-synthesis-independent recovery. However, this experiment demonstrated that the presence of bicarbonate did not prevent photodamage and therefore the effect of PS II-specific electron acceptors on PS II activity in the Δ(E13–N15) and Y20A mutants was investigated (also see Fig. S2).

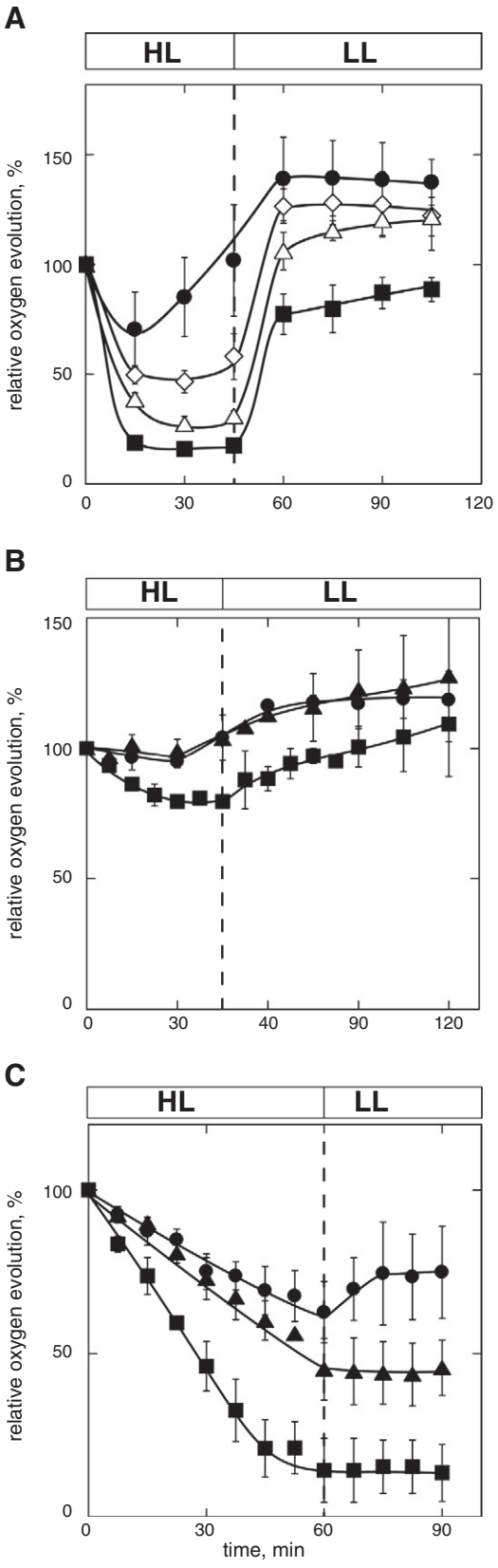

3.5. Sensitivity to artificial quinones in the Δ(E13–N15) and Y20A cells

Oxygen evolution rates shown in Table 1 indicated that even without high-light treatment DMBQ/$K_3Fe(CN)_6$-supported oxygen-evolving activity of the Δ(E13–N15) cells was impaired compared to activity in the presence of bicarbonate. In contrast, the wild type and the Δ(N6–N8), Δ(P11–V12) and Y20A cells had similar rates with either electron sink (Table 1). To investigate the impact of DMBQ on PS II activity in the Δ(E13–N15) strain, oxygen evolution at different concentrations of DMBQ was measured. As shown in Fig. 5A, the Δ(E13–N15) cells were sensitive towards DMBQ with a half-inhibitory concentration (I_{50}) of 225 μM; and the addition of 400 μM DMBQ resulted in ~70% reduction of oxygen-evolving activity. In contrast, DMBQ enhanced oxygen evolution in the wild type and resulted in a linear increase in oxygen evolution rates with a two-fold increase at 400 μM of DMBQ relative to the activity in the absence of DMBQ. In contrast, Y20A cells were not responsive to increasing the concentration of DMBQ.

The Δ(E13–N15) cells were also sensitive to 2,6-dichlorobenzoquinone (DCBQ) concentrations with an I_{50} value of 50 μM (Fig. 5B); however, although the rate fluctuated at higher DCBQ concentrations it did not decrease further. Moreover, Y20A cells exhibited little change with increasing concentrations of DCBQ and no inhibitory effect was observed in the wild type where an observed stimulation of oxygen-evolving activity saturated at 200 μM.

3.6. Fluorescence induction is altered in the Δ(E13–N15) strain in the presence of DMBQ

To investigate the effect of DMBQ on electron transfer through PS II in the Δ(E13–N15) cells, steady-state chlorophyll *a* fluorescence induction measurements were made in the presence and absence of DMBQ with the omission of $K_3Fe(CN)_6$. Upon turning on the actinic light the variable fluorescence rises to an initial J level that corresponds to reduction of Q_A and then, following an intermediate plateau (I), the fluorescence increases to a maximum P level. The fluorescence then declines as a result of the activation of Calvin–Benson cycle enzymes and the various quenching mechanisms [35–38]. In Fig. 6, total variable fluorescence yield in the Δ(E13–N15) cells is lower than in the wild type reflecting the reduced level of active PS II centers in this mutant; however, the ratio of the O to J rise divided by the I to P rise is larger in the Δ(E13–N15) strain indicating that there is an accumulation of reduced Q_A in these cells (Fig. 6A, B). Both the wild type and the Δ(E13–N15) cells were inhibited by the addition of diuron that prevents oxidation of Q_A^- by binding at the Q_B site [39]. The addition of DMBQ to the wild type caused some alteration of the fluorescence induction kinetics but the changes did not suggest impairment of electron transfer. In contrast,

Fig. 4. Oxygen evolution of light-stressed PsbL mutant cells in the presence of difference electron acceptors. (A) Oxygen evolution measured in the presence of 200 μM DMBQ and 1 mM $K_3Fe(CN)_6$. Wild type (closed circles); Δ(N6–N8) (open diamonds); Δ(P11–V12) (open triangles); Δ(E13–N15) (closed squares). (B) Sensitivity of the Δ(E13–N15) and ϒ20A strains in the presence of 15 mM sodium bicarbonate. Wild type (closed circles); Δ(E13–N15) (closed squares); Y20A (closed triangles). (C) Response of wild-type and mutant cells to high light in the presence of kanamycin and 15 mM sodium bicarbonate. Symbols are the same as in panel B. Kanamycin at 50 μg mL^{-1} was added at the beginning of the experiment. In panels A–C, high light (HL) was 2000 μmol photons m^{-2} s^{-1} and low light (LL) was 30 μmol photons m^{-2} s^{-1}. Oxygen evolution data are the average ± the standard error from three independent experiments.

Table 1
Rates of oxygen evolution (μmol O_2(mg chlorophyll)$^{-1}$ h^{-1}) in *Synechocystis* sp. PCC 6803 cells of the wild type and the PsbL N-terminal deletion mutants as measured in the presence of different electron acceptors.

Electron acceptors	Wild type	Control	Δ(N6–N8)	Δ(P11–V12)	Δ(E13–N15)	Y20A
No addition	403 ± 22	451 ± 54	450 ± 23	439 ± 7	428 ± 37	470 ± 38
DMBQ[a]	658 ± 2	660 ± 20	513 ± 33	663 ± 15	189 ± 43	633 ± 18
Bicarbonate[b]	653 ± 38	n.d.[c]	n.d.	n.d.	581 ± 65	587 ± 45

[a] Electron acceptors were 200μM DMBQ and 1mM $K_3Fe(CN)_6$.
[b] Sodium bicarbonate at 15mM was added to support oxygen evolution.
[c] n.d.: not determined.

addition of DMBQ to the Δ(E13–N15) cells induced a marked change in the fluorescence induction trace which more closely resembled the addition of the herbicide. These data suggest that the acceptor side of PS II is altered in the Δ(E13–N15) cells so as to slow electron transfer between Q_A^- and Q_B and that this change is accompanied by DMBQ acting in a similar fashion to diuron and blocking forward electron transfer in the mutant.

We also investigated the fluorescence induction profile from the Y20A mutant with no addition or in the presence of diuron and the kinetics resembled those observed for the wild type; however, the total variable fluorescence yield was reduced (Fig. 7C). The addition of DMBQ to the Y20A cells resulted in a fluorescence profile that plateaued earlier than that of the wild type but unlike the Δ(E13–N15) strain this did not resemble the addition of diuron.

The increase of fluorescence at 1 s in the presence of diuron in both the wild type and the mutants was not investigated further in this study (but see [40]); however, the extent of the variable fluorescence observed in the presence of diuron in Fig. 6A, B suggests that there is a two-fold reduction in the relative level of PS II in the Δ(E13–N15) cells compared to the wild type. This conclusion is supported by the extent of variable fluorescence observed for the control and the Δ(E13–N15) cells after a single-turnover actinic flash in Fig. 7 (see below) and hence suggests that the herbicide-binding assay may have underestimated the level of assembled PS II centers in the mutant (cf. Fig. 2D).

3.7. Flash-induced chlorophyll a fluorescence relaxation

To test the hypothesis that DMBQ acts to block Q_A^- oxidation in the Δ(E13–N15) cells, the decay kinetics of the variable chlorophyll *a* fluorescence yield were measured after a saturating flash. Fig. 7A, B present primary data from the wild type and the Δ(E13–N15) cells on a log scale: Fig. 7C, D present the normalized data with the inset showing the decay on a linear scale for 10 ms after the actinic flash. The kinetics can be divided into three components: a fast phase ascribed to forward electron transfer from Q_A^- to Q_B, an intermediate phase describing the binding of plastoquinone to the Q_B site, and one slow phase ascribed to a back reaction consisting of charge recombination between Q_A^- and the donor side of PS II [29,41,42].

In the absence of DMBQ, the fluorescence yield relaxation in the control was dominated by a fast phase (half time, ~270 μs) with an amplitude of ~60%. The contribution of the intermediate phase (half time, ~2.5 ms) was ~35% and the slow phase (half time, ~8.0 s) had an amplitude of ~5% (Table 2). In the Δ(E13–N15) cells, the decay kinetics resembled those of the control except the half time of the fast phase which was ~300 μs and corresponded to ~50% of the total fluorescence amplitude and there was also a factor of two increase in the rate and amplitude of the slow component.

When DMBQ was present there was little effect on the chlorophyll *a* fluorescence decay kinetics of the control beyond a small acceleration of the fast phase and a slowing of the intermediate phase from 2.5 ms to 3.2 ms (Table 2). In contrast, addition of DMBQ to the Δ(E13–N15) cells slowed the fast and intermediate phases and reduced their amplitudes. The presence of DMBQ also accelerated the rate of the slow phase from 4.0 s to 1.3 s and increased the amplitude of this component from 15 to 45%. These results suggest that DMBQ slows forward electron transfer and enhances the back reaction with the S_2 state of the OEC in the Δ(E13–N15) cells (for a discussion of the S states of the OEC, see [1]). Moreover, these observations support the interpretation that the

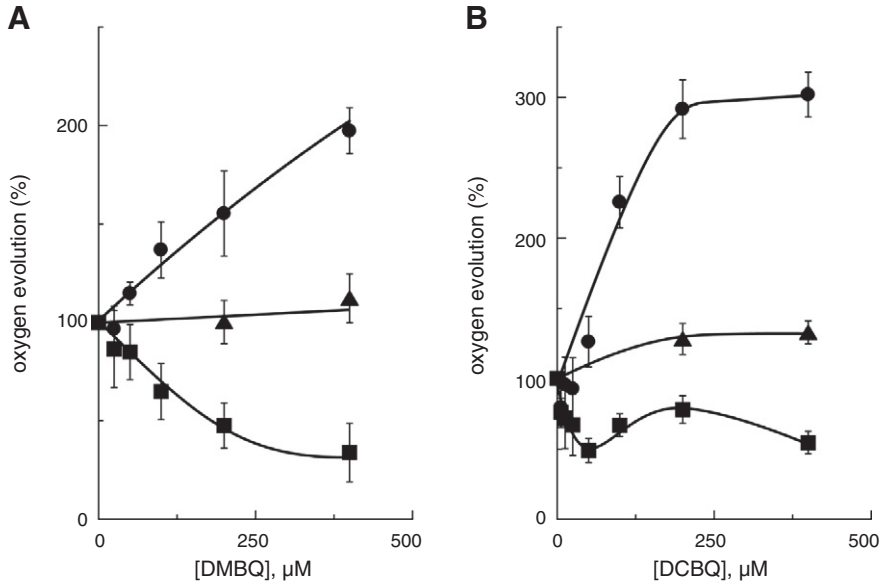

Fig. 5. Effect of artificial quinones on oxygen evolution in wild type and mutant strains. Oxygen evolution was measured using DMBQ (A) or DCBQ (B) as an electron acceptor in wild type (circles), Δ(E13–N15) (squares) and Y20A (triangles). Oxygen evolution was measured at saturating light intensity in the presence of 1 mM $K_3Fe(CN)_6$ to keep quinones oxidized. Data are the average ± the standard error from at least three independent experiments.

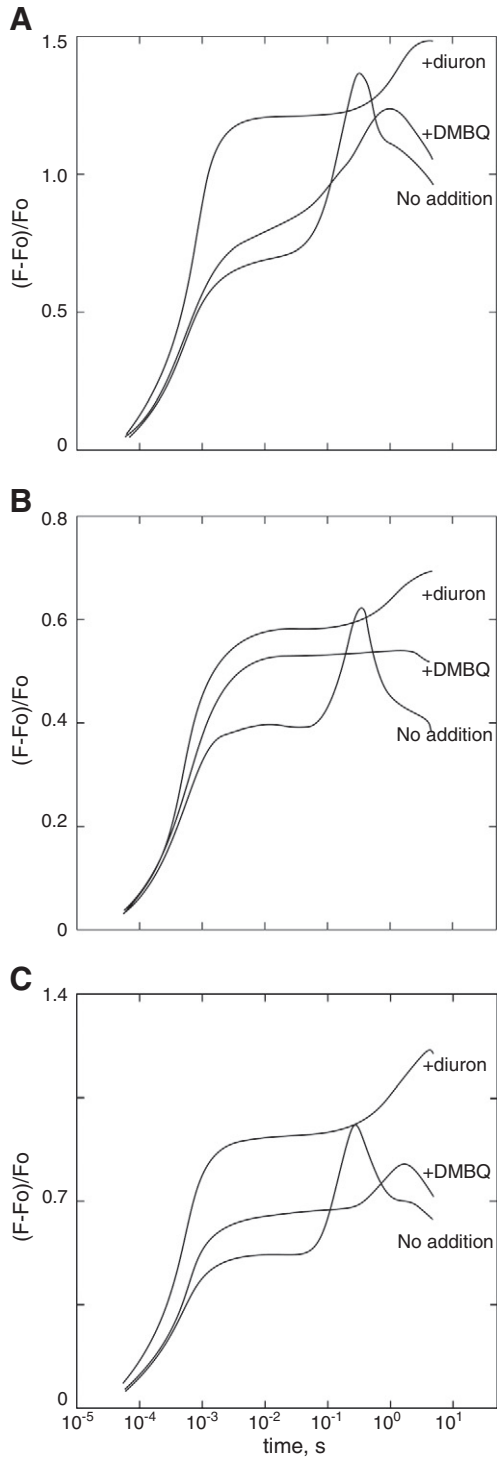

Fig. 6. Fluorescence induction in intact cells. Normalized florescence induction curves of wild type (A), Δ(E13–N15) (B), and Y20A (C) in the absence or presence of 40 μM diuron or in the presence of 0.2 mM DMBQ. The light intensity was 2800 μmol photons m^{-2} s^{-1} with the excitation maxima at 455 nm.

Q_B site in the Δ(E13–N15) strain is altered and that DMBQ may have displaced bound plastoquinone.

Since the Y20A cells were also sensitive to DMBQ, although the inhibitory effect required exposure to high light [24], we also determined the effect of DMBQ on the variable chlorophyll *a* fluorescence decay kinetics in this mutant. The cells were subjected to similar light stress conditions as seen in Fig. 4 and the cells were harvested at the specified time points and their fluorescence decay kinetics measured (Table 3 and Fig. 8). In wild type, prolonged irradiation for 45 min led to ~50% reduction in the total variable fluorescence yield indicating light-induced reduction of functional Q_A. However, when compared to non-irradiated cells, the slow phase of the fluorescence decay was accelerated from ~6.0 to ~1.0 s and the relative contribution of this phase was increased from ~9 to ~20% with a corresponding reduction in the amplitude of the fast phase (Table 3). This suggests that a sizable fraction of the remaining Q_A active centers following high-light-induced stress was transformed into non-Q_B-reducing centers and underwent a back reaction with the PSII donor side. However, the half times of the fast and intermediate phases remained essentially unaltered. Moreover, the response of the Y20A cells following high-light-induced stress was similar to the wild type except that there was an ~70% reduction in the total variable fluorescence following high-light exposure for 45 min (Table 3).

When DMBQ was added to wild-type cultures following high-light-induced stress, the fluorescence decay kinetics remained dominated by the fast phase, as they had been in the absence of DMBQ, corresponding to almost 50% of the total amplitude after 45 min illumination, with a half time of ~180 μs. Also, after the high-light treatment, the amplitude of the intermediate and slow phases was 25% and 28% and their half times were 3.3 ms and 1.8 s, respectively. In contrast, following the 45 min high-light-induced stress, the kinetics of the chlorophyll *a* variable fluorescence decay in the Y20A cells were dominated by the slow phase (half time, 1.7 s) with an amplitude of ~45%: while that of the fast phase was reduced to 36%. Additionally, in the Y20A cells, the amplitude of the intermediate phase remained essentially unchanged but the half time was more than two-fold longer (6.9 ms vs. 2.5 ms) compared to cells in the absence of DMBQ but after exposure to high light for 45 min (Table 3).

These data suggest that DMBQ may impair forward electron transfer in the light-stressed Y20A cells in a similar manner to DMBQ-induced inhibition of Q_A^- oxidation in the non-light-stressed Δ(E13–N15) cells. Moreover, the apparent increase in the amplitude of the back reaction corresponding to charge recombination between Q_A^- and the PS II donor side, together with the observed increase in the rate of the intermediate component in the Y20A cells, suggests that this mutant may also possess an altered Q_B site following light-induced stress that can be perturbed by DMBQ.

3.8. Oxygen evolution as a function of PS II herbicide concentration in wild type and the PsbL mutant cells

Since the oxygen-evolving rates measured with no addition or in the presence of bicarbonate in the Δ(E13–N15) and Y20A strains were similar to those of the wild type (Fig. 2C, Table 1), this could be explained by plastoquinone accessing the Q_B site normally under physiological conditions. On the other hand, our herbicide-binding data and chlorophyll *a* fluorescence yield measurements suggest that the affinity of plastoquinone to the Q_B site may be affected in these mutants. To explore these ideas, oxygen evolution in whole cells was measured in the presence of atrazine, diuron and bromoxynil, examples of triazine, urea and phenolic herbicides, respectively, which all bind to the Q_B niche of PS II [43–46]. Fig. 9 shows that PS II activity in the mutant strains was readily inhibited by lower concentrations of atrazine and diuron compared to the wild type (Fig. 9A, B). In the Δ(E13–N15) mutant, the I_{50} value of atrazine was 2.5 μM, while the I_{50} in the wild type was 11 μM (Table 4). The Y20A cells exhibited a similar I_{50} value as that of the Δ(E13–N15) mutant at 2.0 μM. The I_{50} of diuron in the wild type was 750 nM, and those of the Δ(E13–N15) and Y20A strains were 330 nM and 350 nM, respectively. Interestingly, the Y20A cells exhibited a similar sensitivity to the phenolic herbicide bromoxynil as that of the wild type (I_{50} values of 120 μM and 100 μM for the wild-type and Y20A cells, respectively) but the Δ(E13–N15) cells were found to have an I_{50} value of 25 μM (Fig. 9C, Table 4). In addition, the I_{50} of atrazine in the wild-type thylakoids was 760 nM but ~280 nM in the two mutants (Fig. S3).

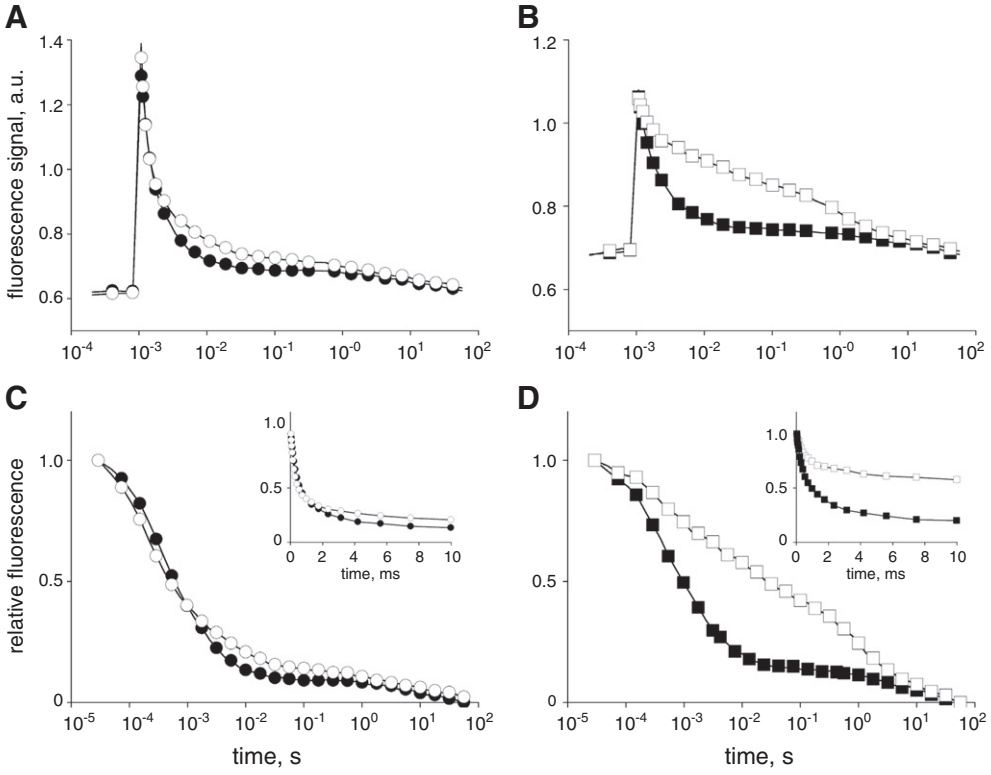

Fig. 7. Relaxation of flash-induced chlorophyll *a* fluorescence in the control strain (A) and the Δ(E13–N15) strain (B) in the absence or presence of DMBQ. (A, B) Decay of variable fluorescence yield after cells were excited with a single turnover saturating flash (455 nm light) at t = 1 ms. Control -DMBQ (closed circles), control +DMBQ (open circles), Δ(E13-N15) -DMBQ (closed squares), Δ(E13-N15) +DMBQ (open squares). (C, D) Normalized plot of the decay of variable fluorescence yield from panel A. Symbols as in panels A and B. The insets show changes of the fluorescence signals over the initial 10 ms on a linear scale. Signals were normalized to the initial fluorescence yield following the actinic flash. Results are the average of three independent measurements. For clarity only every second data point is shown.

4. Discussion

Removal of PsbL in *Nicotiana tabacum* (tobacco) has been reported to result in impaired biosynthesis of PS II to a level where photoautotrophic growth is not supported [47,48]. A similar phenotype was obtained with Δ*psbL* mutants of *Synechocystis* 6803 and these results suggest that association of CP43 with the CP43-less PS II subcomplex is impeded [21,22,48]. Where functional PS II centers were assembled in Δ*psbL* tobacco mutants, the Q_B binding site was perturbed so as to facilitate backward electron flow from PQH_2 to Q_A [20]. Truncation of the four membrane-embedded C-terminal residues of PsbL in *Synechocystis* 6803 also prevented PS II assembly and led to an accumulation of the CP43-less PS II subcomplex [24]. PsbL is characterized by an ~24 amino acid membrane-spanning segment and an ~15 amino acid hydrophilic extension on the cytosolic side of the membrane that is unique among the membrane-spanning LMW subunits of PS II. The Δ(N6–N8), Δ(P11–V12) and Δ(E13–N15) mutants of this study all target this hydrophilic region (Fig. 1).

The interactions of the N-terminal extension with neighboring PS II subunits in the 1.9-Å resolution PS II structure (PDB ID: 3ARC) from *T. vulcanus* are summarized in Fig. 10 (numbering here is for *T. vulcanus*, cf. Fig. 1 and Supplementary Fig. S1 which shows the N-terminal two-amino-acid deletion with respect to the sequence for PsbL from *Synechocystis* 6803). The PsbL hydrophilic segment may stabilize the Q_B-binding site via interactions with the D–E loop of D1 through interactions with the N-terminus of CP47. In the *T. vulcanus* structure the PsbL residues Asn-6, Pro-9 and Glu-11 make hydrogen bonds with the CP47 residues Asp-15, Leu-3 and Gly-2, respectively (Fig. 10). The CP47 residues Leu-3 and Arg-7 hydrogen bond with Thr-230 and Glu-231 of the D1 D–E loop which, in turn, connects to the quinone–Fe complex through D1-His-215. Hence disruption of these interactions might result in a structural change in the vicinity of the Q_B-binding site by perturbing D1-His-215.

An involvement of the D–E loop in the conformation of the Q_B site has been previously investigated through the introduction of long deletions in this region of D1 [33,49]. Notably the D1:Δ(R225-F239) mutant was found to exhibit lower rates of oxygen evolution when supported by DMBQ than when supported by DCBQ but had similar rates to a control strain when oxygen evolution was supported by the addition of bicarbonate [49]. Interestingly, the short deletion between Glu13 and Asn-15 in the hydrophilic extension of PsbL produced a similar phenotype whereby rates of oxygen evolution were close to the control value in the presence of bicarbonate (Table 1) but were suppressed when DCBQ or DMBQ were used as an electron acceptor (Fig. 4). In contrast to the D1:Δ(R225-F239) mutant, however, the PsbL:Δ(E13–N15) cells were more susceptible to partial inhibition by DCBQ than DMBQ.

Among the three PsbL deletion strains, the Δ(E13–N15) mutant possessed the most severe phenotype and this would be expected since the corresponding Asn in *T. vulcanus* (Asn-13) is hydrogen bonded to Ser-16 as a result of the register of the membrane-spanning helix. Since the register of the helix is unlikely to change due to the multiple

Table 2
Effect of DMBQ on forward electron transfer kinetics in cells of the *Synechocystis* sp. PCC 6803 PsbL control strain and the PsbL Δ(E13–N15) mutant.

Strain	Fast phase $t_{1/2}$ (μs)/Amp (%)	Intermediate phase $t_{1/2}$ (ms)/Amp (%)	Slow phase $t_{1/2}$ (s)/Amp (%)
Control			
No addition:	274 ± 10/60 ± 1	2.5 ± 0.1/35 ± 1	8.3 ± 0.7/7 ± 0.1
DMBQ:	209 ± 9/63 ± 1	3.2 ± 0.4/28 ± 1	6.2 ± 0.9/13 ± 0.4
Δ(E13–N15)			
No addition:	303 ± 19/52 ± 2	3.0 ± 0.2/34 ± 2	4.0 ± 0.5/15 ± 0.3
DMBQ:	390 ± 34/30 ± 1	12.4 ± 1.3/24 ± 1	1.3 ± 0.1/45 ± 0.7

Table 3
Effect of DMBQ on relaxation of the flash-induced chlorophyll *a* fluorescence yield in *Synechocystis* sp. PCC 6803 wild type and the PsbL Y20A strain following exposure to high light.[a]

Strain	Time (min)	Total amplitude (%)	Fast phase $t_{1/2}$ (μs)/Amp (%)	Intermediate phase $t_{1/2}$ (ms)/Amp (%)	Slow phase $t_{1/2}$ (s)/Amp (%)
wild type	0	100	280 ± 12/64 ± 1	2.3 ± 0.2/31 ± 2	6.3 ± 0.8/9 ± 0.2
	15	67	278 ± 17/50 ± 2	2.5 ± 0.2/32 ± 2	1.9 ± 0.1/18 ± 0.3
	30	56	305 ± 25/49 ± 2	2.7 ± 0.3/27 ± 2	1.2 ± 0.1/23 ± 0.4
	45	50	285 ± 20/51 ± 2	2.6 ± 0.3/29 ± 2	1.6 ± 0.1/20 ± 0.3
Y20A	0	100	325 ± 14/61 ± 2	3.0 ± 0.2/30 ± 2	6.8 ± 0.8/12 ± 0.2
	15	59	336 ± 21/51 ± 2	3.2 ± 0.4/25 ± 2	1.6 ± 0.1/24 ± 0.4
	30	40	286 ± 24/50 ± 2	3.0 ± 0.4/28 ± 2	2.2 ± 0.2/21 ± 0.5
	45	28	205 ± 18/48 ± 2	2.5 ± 0.3/32 ± 2	1.6 ± 0.2/20 ± 0.5
wild type +DMBQ	0	100	180 ± 10/64 ± 1	4.4 ± 0.4/26 ± 1	4.2 ± 0.6/15 ± 0.4
	15	71	212 ± 12/56 ± 1	4.7 ± 0.4/25 ± 1	2.7 ± 0.2/22 ± 0.4
	30	52	209 ± 12/50 ± 1	4.1 ± 0.4/25 ± 1	2.6 ± 0.2/26 ± 0.3
	45	48	184 ± 13/49 ± 1	3.3 ± 0.3/25 ± 1	1.8 ± 0.1/28 ± 0.4
Y20A +DMBQ	0	100	248 ± 16/56 ± 1	5.8 ± 0.7/25 ± 1	2.7 ± 0.3/22 ± 0.5
	15	62	257 ± 16/41 ± 1	5.5 ± 0.5/23 ± 1	1.8 ± 0.1/36 ± 0.4
	30	41	167 ± 18/35 ± 2	5.1 ± 0.7/20 ± 1	1.7 ± 0.1/43 ± 0.6
	45	30	170 ± 22/36 ± 2	6.9 ± 1.3/20 ± 1	1.7 ± 0.1/45 ± 0.1

[a] Cyanobacterial cells were exposed to high light of 2000μmol photons m^{-2} s^{-1} for the indicated amount of time and the relaxation of the flash-induced chlorophyll *a* variable fluorescence yield was measured in the absence or presence of DMBQ.

hydrophobic interactions involved, the interactions involving CP47 are likely to be disrupted in the Δ(E13–N15) mutant. However, the Δ(N6–N8) strain has only one disrupted interaction with CP47 and the Δ(P11–V12) strain may still have interactions between PsbL and CP47 since half of the interactions do not arise from the side chains and may therefore be compensated for in part by the main chain interactions arising in any rearrangement. Nevertheless, we did observe that the structural change introduced into the Δ(N6–N8) mutant prevented recognition by our PsbL antibody whereas PsbL in the other strains was readily detected (Fig. 2A).

The different extent of the conformational change expected in the mutants might also explain their different impacts on dimer formation observed in Fig. 3. These experiments were performed in the presence of 1% n-dodecyl β-D-maltoside (DM). However, biochemical characterization in *T. elongatus* and *Synechocystis* 6803 suggests that addition of DM induces the formation of dimeric PS II complexes [50,51]: thus our data imply that dimer stability is reduced in the Δ(P11–V12) and Δ(E13–N15) mutants.

Both the measurements of variable chlorophyll *a* induction and the decay of chlorophyll fluorescence following a single turnover actinic

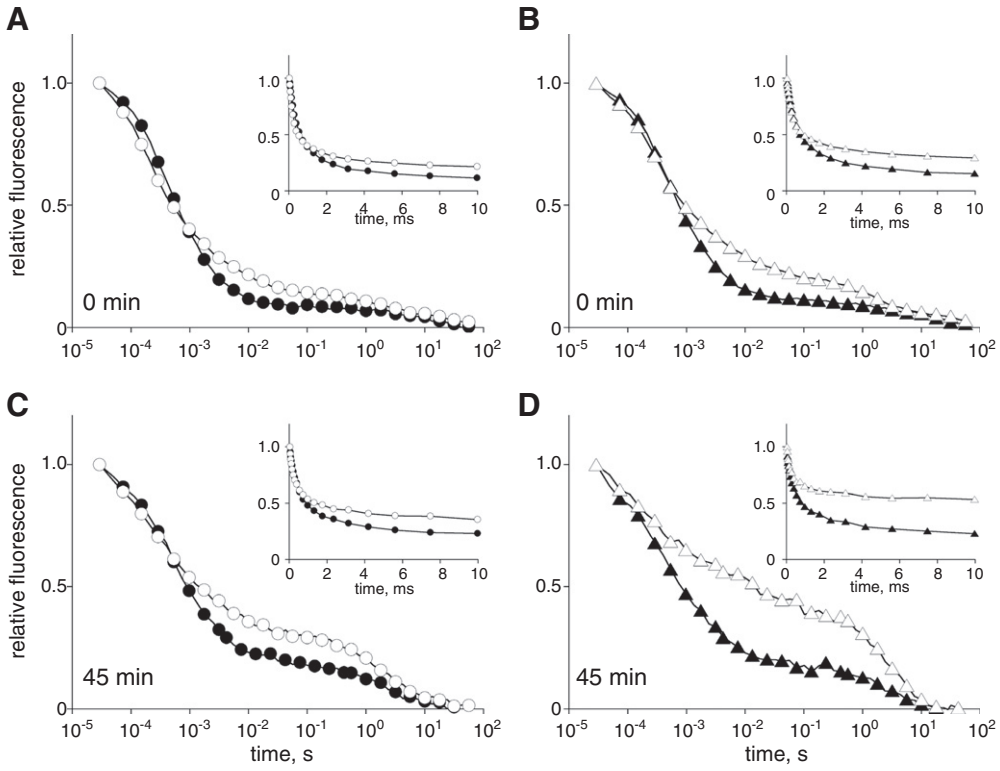

Fig. 8. Comparison of flash-induced chlorophyll *a* fluorescence relaxation measurements in the wild type and the Y20A strain in the presence or absence of DMBQ after high-light pre-illumination. Symbols are wild type (circles) and Y20A (triangles). (A) Non-irradiated wild-type cells. (B) Non-irradiated Y20A cells. (C) Light-treated wild-type cells after 45 min pre-illumination. (D) Light-treated Y20A cells after 45 min pre-illumination. The insets show changes of the fluorescence signals over the initial 10 ms on a linear scale. When pre-illuminated, the light intensity was 2000 μmol photons m^{-2} s^{-1}. Decay traces with DMBQ are in open symbols, and without DMBQ are in closed symbols. Signals were normalized to the initial fluorescence yield following an actinic flash. For clarity only every second data point is shown.

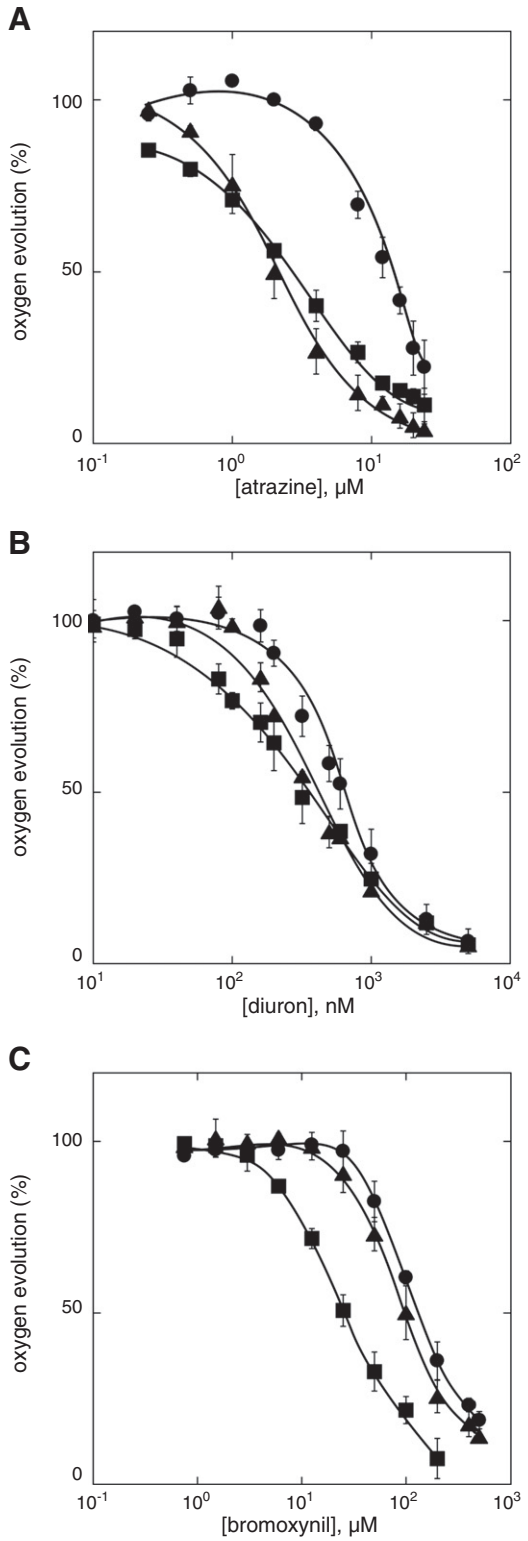

Fig. 9. Determination of the concentration of herbicide required to reduced initial PS II activity by 50% (I_{50}) for atrazine (A), diuron (B) and bromoxynil (C) in wild type and the mutant cells as measured by oxygen evolution. Symbols are: wild type (circles), Δ(E13–N15) (squares) and Y20A (triangles). Oxygen evolution was measured at saturating light intensity in the absence of artificial electron acceptors. Data are the average ± the standard error from at least three independent experiments.

flash in the presence and absence of DMBQ indicated that the Q_B-binding site was altered in the Δ(E13–N15) strain. Interestingly, the back reaction with the donor side of PS II in the presence of diuron was not affected (Supplementary Fig. S4) suggesting that there was no apparent change associated with the Q_A-binding site or midpoint potential of the Q_A/Q_A^- couple. That the Q_B-site was specifically targeted was corroborated by the approximately two-fold increase in the K_D for atrazine in the herbicide-binding assay (Fig. 2D). This was further supported by the increased sensitivity of oxygen evolution in this strain to all three classes of herbicide clearly suggesting an altered binding environment (Figs. 9 and S3; Table 4) and by the varied effects of DMBQ and DCBQ on oxygen evolution in the Δ(E13–N15) and wild-type cells. Since the Q_B-binding site turns over after two actinic flashes we also measured the impact of DMBQ on the decay of chlorophyll fluorescence as a function of single turnover flashes spaced at 200 ms (Supplementary Fig. S5 and S6). The inhibition was increased after the second flash and remained inhibited to a similar extent out to five turnovers suggesting that the two-electron gate was inoperable in the presence of DMBQ in the Δ(E13–N15) cells.

Table 4
Half-inhibitory concentrations of herbicide in cells of *Synechocystis* sp. PCC 6803 wild type and the PsbL Δ(E13–N15) and Y20A mutants as determined by measuring oxygen evolution.[a]

Strain	$I_{50}^{atrazine}$ (μM)	I_{50}^{diuron} (nM)	$I_{50}^{bromoxynil}$ (μM)
Wild type	11.0	750	120
Δ(E13–N15)	2.5	330	25
Y20A	2.0	350	100

[a] The rates of oxygen evolution from cyanobacteria cells were measured in the absence of electron acceptors.

The Δ(E13–N15) mutant was highly susceptible to photodamage (Fig. 4). This is also consistent with the proposed disruption of the Q_B-binding environment through conformational changes relayed between CP47, the D–E loop of D1 and His-215 of D1 as depicted in Fig. 10 [52,53]. A comparison was made between the Δ(E13–N15) cells and the Y20A cells as the Y20A mutant was sensitive to photodamage [24]. Typically the phenotype of the Y20A was less severe than that of the Δ(E13–N15) cells in the various assays and in particular the Y20A cells retained the same sensitivity as that of the wild type towards the phenolic herbicide bromoxynil and displayed a different dependence on the exogenous electron acceptors DMBQ and DCBQ in oxygen evolution assays (Fig. 5). These results suggest that the Q_B-binding environment in the Y20A cells, although altered from the wild type, was distinct from that in the Δ(E13–N15) mutant.

The D1:Δ(R225-F239) strain discussed above and the PsbL:Δ(E13–N15) strain differ in their susceptibility to photodamage. In the presence of DMBQ, oxygen evolution was rapidly inactivated in both mutants; however, in the presence of bicarbonate D1:Δ(R225-F239) cells were rapidly photodamaged but the PsbL:Δ(E13–N15) strain was not. Our data in Fig. 4B, C demonstrated that the ability of PsbL:Δ(E13–N15) (and Y20A) cells to tolerate high-light-induced stress in the presence of bicarbonate was dependent on protein synthesis but the control strain exhibited protein-synthesis-independent recovery. Protein-synthesis-independent recovery was also reported for the D1:Δ(R225-F239) mutant following photodamage in the presence of bicarbonate and it was suggested that this recovery represents an initial reversible component of photodamage associated with changes in the vicinity of the Q_B-binding site in the D1:Δ(R225-F239) strain [49]. Although seen in our control and in D1:Δ(R225-F239) cells, protein-synthesis-independent recovery was not observed in the PsbL:Δ(E13–N15) and Y20A mutants. This suggests that the disruption of the Q_B site in PsbL:Δ(E13–N15) cells, and in the Y20A strain, induced a greater susceptibility to photodamage than the 14-amino-acid deletion seen in the D1:Δ(R225-F239) mutant. Moreover, in the study by Mulo and co-workers [49] protein-synthesis-independent recovery from photodamage was not observed in their control that only retained the *psbA2* gene from the three copies of *psbA* found in *Synechocystis* 6803. Thus the ability of wild-type cells to adapt to high-light-induced stress, and to exhibit the initial reversible component of

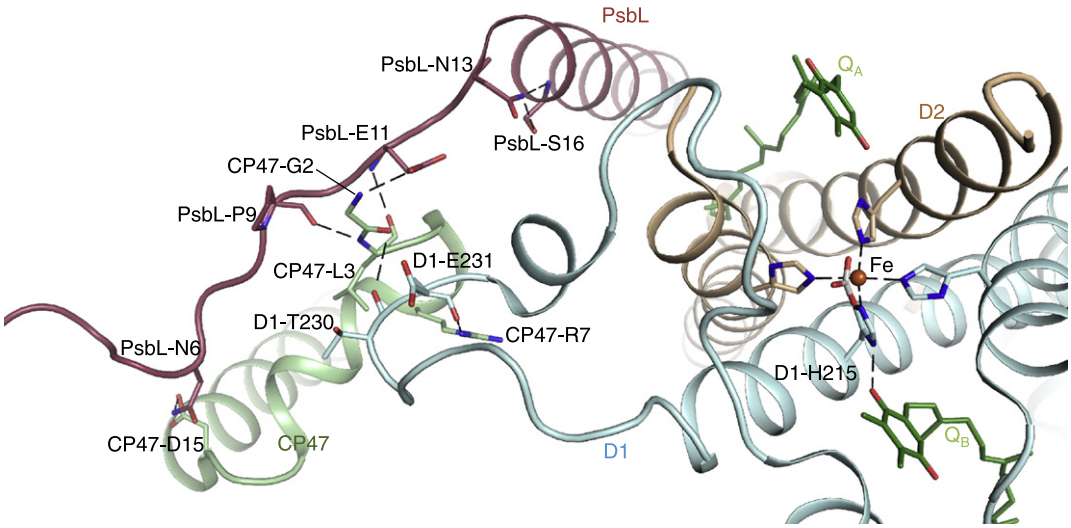

Fig. 10. Model of the interactions of the N-terminus of PsbL with CP47 and D1 on the acceptor side of PS II. The data are from PDB ID: 3ARC [5] and depict the acceptor side of PS II from *Thermosynechococcus vulcanus* and the numbering system shown is for this cyanobacterium. *T. vulcanus* has a two-amino-acid deletion in PsbL with respect to *Synechocystis* sp. PCC 6803 and has the same sequence and numbering as *T. elongatus* (Fig. 1 and Supplementary Fig. S1). The figure was displayed using PyMOL [61].

photodamage under appropriate experimental conditions, may require an active copy of *psbA3* (or even *psbA1*) [54–56].

The equivalent Tyr to *Synechocystis* 6803 Tyr-20 in *T. vulcanus* is Tyr 18. This residue is hydrogen bonded with the main chain carbonyl oxygen of Phe-19 and Phe-23 of the LMW PsbT subunit and potentially this Tyr also makes hydrophobic interactions with PsbT residues Leu-16 and Ala-20, a sulfoquinovosyldiacylglycerol lipid, and a phosphatidylglycerol molecule (Supplementary Fig. S7–S9). Lipids play distinct structural roles in PS II (reviewed in [57,58]) and blocking the synthesis of phosphatidylglycerol has been shown to block Q_A to Q_B electron transfer in *Synechocystis* 6803 [59,60]: while deletion of PsbT also slowed Q_A to Q_B electron transfer [21]. Thus it is likely that mutation at Tyr-20 of PsbL may affect the Q_B-binding site environment through interactions with PsbT and PS II-specific structural lipids.

Altogether, there are three phosphatidylglycerol molecules in the vicinity of Q_A as well as in the proximity to the PsbL and PsbT proteins at the monomer–monomer interface of the PS II dimer, and these are capped by the D–E loop of D1; there is also a further phosphatidylglycerol located in proximity to Q_B. It therefore appears likely that disruption of protein–lipid interactions in the Δ(P11–V12) and Δ(E13–N15) mutants will also contribute to the reduced PS II dimer stability observed in these strains (Supplementary Fig. S10).

We conclude that in addition to the requirement for PsbL to be bound to the CP43-less subcomplex so as to ensure correct assembly of PS II, the N-terminal hydrophilic region of PsbL modifies the Q_B-binding environment. This interaction may be relayed through PsbL interactions with CP47 that influence the D–E loop of D1. Disruption of these interactions by the introduction of short deletions decreases the affinity of the Q_B-binding site for Q_B but increases the affinity for PS II-directed herbicides and results in the PS II-specific electron acceptor DMBQ becoming an effective inhibitor of forward electron transfer. Mutations at Tyr-20 may also affect the Q_B-binding environment via interactions involving PsbT and PS II structural lipids.

Acknowledgements

This work was supported by a grant (UOO043) from the New Zealand Marsden Fund to J.J.E.-R.

Appendix A. Supplementary data

Supplementary data to this article can be found online at http://dx.doi.org/10.1016/j.bbabio.2014.02.015.

References

[1] G. Renger, Photosynthetic water splitting: apparatus and mechanism, in: J.J. Eaton-Rye, B.C. Tripathy, T.D. Sharkey (Eds.), Photosynthesis: Plastid Biology, Energy Conversion and Carbon Assimilation, Advances in Photosynthesis and Respiration, vol. 34, Springer, Dordrecht, 2012, pp. 359–411.
[2] D.J. Vinyard, G.M. Ananyev, G.C. Dismukes, Photosystem II: the reaction center of oxygenic photosynthesis, Annu. Rev. Biochem. 82 (2013) 577–606.
[3] K.N. Ferreira, T.M. Iverson, K. Maghlaoui, J. Barber, S. Iwata, Architecture of the photosynthetic oxygen-evolving center, Science 303 (2004) 1831–1838.
[4] B. Loll, J. Kern, W. Saenger, A. Zouni, J. Biesiadka, Towards complete cofactor arrangement in the 3.0 Å resolution structure of Photosystem II, Nature 438 (2005) 1040–1044.
[5] Y. Umena, K. Kawakami, J.-R. Shen, N. Kamiya, Crystal structure of oxygen-evolving Photosystem II at a resolution of 1.9 Å, Nature 473 (2011) 55–60.
[6] A. Guskov, J. Kern, A. Gabdulkhakov, M. Broser, A. Zouni, W. Saenger, Cyanobacterial Photosystem II at 2.9-Å resolution and the role of quinones, lipids, channels and chloride, Nat. Struct. Mol. Biol. 16 (2009) 334–342.
[7] J. Deisenhofer, O. Epp, I. Sinning, H. Michel, Crystallographic refinement at 2.3 Å resolution and refined model of the photosynthetic reaction centre from *Rhodopseudomonas viridis*, J. Mol. Biol. 246 (1995) 429–457.
[8] A. Trebst, The topology of the plastoquinone and herbicide binding peptides of Photosystem II in the thylakoid membrane, Z. Naturforsch. 41c (1986) 240–245.
[9] W.D. Schubert, O. Klukas, W. Saenger, H.T. Witt, P. Fromme, N. Kraus, A common ancestor for oxygenic and anoxygenic photosynthetic systems: a comparison based on the structural model of Photosystem I, J. Mol. Biol. 280 (1998) 297–314.
[10] A.W. Rutherford, A. Osyczka, F. Rappaport, Back-reactions, short-circuits, leaks and other energy wasteful reactions in biological electron transfer: redox tuning to survive life in O_2, FEBS Lett. 586 (2012) 603–616.
[11] J. Raymond, R.E. Blankenship, The evolutionary development of the protein complement of Photosystem 2, Biochim. Biophys. Acta 1655 (2004) 133–139.
[12] T.M. Bricker, J.L. Roose, R.D. Fagerlund, L.K. Frankel, J.J. Eaton-Rye, The extrinsic proteins of Photosystem II, Biochim. Biophys. Acta 1817 (2012) 121–142.
[13] J. Nickelsen, B. Rengstl, Photosystem II assembly: from cyanobacteria to plants, Annu. Rev. Plant Biol. 64 (2013) 609–635.
[14] L.-X. Shi, W.P. Schröder, The low molecular mass subunits of the photosynthetic supracomplex, Photosystem II, Biochim. Biophys. Acta 1608 (2004) 75–96.
[15] L.E. Thornton, J.L. Roose, H.B. Pakrasi, The low molecular weight components, in: T.J. Wydrzynski, K. Satoh (Eds.), Photosystem II: The Light-driven Water:Plastoquinone Oxidoreductase, Advances in Photosynthesis and Respiration, vol. 22, Springer, Dordrecht, 2005, pp. 121–138.
[16] F. Müh, T. Renger, A. Zouni, Crystal structure of cyanobacterial Photosystem II at 3.0 Å resolution: a closer look at the antenna system and the small membrane-intrinsic subunits, Plant Physiol. Biochem. 46 (2008) 238–264.
[17] L.-X. Shi, M. Hall, C. Funk, W.P. Schröder, Photosystem II, a growing complex: updates on newly discovered components and low molecular mass proteins, Biochim. Biophys. Acta 1817 (2012) 13–25.
[18] R.E. Regel, N.B. Ivleva, H. Zer, J. Meurer, S.V. Shestakov, R.G. Herrmann, H.B. Pakrasi, I. Ohad, Deregulation of electron flow within Photosystem II in the absence of the PsbJ protein, J. Biol. Chem. 276 (2001) 41473–41478.
[19] L. Lupinkova, J. Metz, B. Diner, I. Vass, J. Komenda, Histidine residue 252 of the Photosystem II D1 polypeptide is involved in a light-induced cross-linking of the polypeptide with the alpha subunit of cytochrome *b*-559: study of a site-directed mutant of *Synechocystis* PCC 6803, Biochim. Biophys. Acta 1554 (2002) 192–201.

[20] I. Ohad, C.D. Bosco, R.G. Herrmann, J. Meurer, Photosystem II proteins PsbL and PsbJ regulate electron flow to the plastoquinone pool, Biochemistry 43 (2004) 2297–2308.
[21] F.K. Bentley, H. Luo, P. Dilbeck, R.L. Burnap, J.J. Eaton-Rye, Effects of inactivating *psbM* and *psbT* on photodamage and assembly of Photosystem II in *Synechocystis* sp. PCC 6803, Biochemistry 47 (2008) 11637–11646.
[22] P.R. Anbudurai, H.B. Pakrasi, Mutational analysis of the PsbL protein of Photosystem II in the cyanobacterium *Synechocystis* sp. PCC 6803, Z. Naturforsch. 48 (1993) 267–274.
[23] H. Hoshida, R. Sugiyama, Y. Nakano, T. Shiina, Y. Toyoshima, Electron paramagnetic resonance and mutational analyses revealed the involvement of Photosystem II-L subunit in the oxidation step of Tyr-Z by P_{680}^{+} to form the Tyr-$Z^{+}P_{680}Pheo^{-}$ state in Photosystem II, Biochemistry 36 (1997) 12053–12061.
[24] H. Luo, J.J. Eaton-Rye, Directed mutagenesis of the transmembrane domain of the PsbL subunit of Photosystem II in *Synechocystis* sp. PCC 6803, Photosynth. Res. 98 (2008) 337–347.
[25] J.G.K. Williams, Construction of specific mutations in Photosystem II photosynthetic reaction center by genetic engineering methods in *Synechocystis* 6803, Methods Enzymol. 167 (1988) 766–778.
[26] J.J. Eaton-Rye, Construction of gene interruptions and gene deletions in the cyanobacterium *Synechocystis* sp. PCC strain 6803, in: R. Carpentier (Ed.), Photosynthesis Research Protocols, Methods in Molecular Biology, vol. 684, Springer, Humana Press, Totowa, 2011, pp. 295–312.
[27] W. Vermaas, J. Charité, G. Shen, Q_A binding to D2 contributes to the functional and structural integrity of Photosystem-II, Z. Naturforsch. 45c (1990) 359–365.
[28] T.R. Morgan, J.A. Shand, S.M. Clarke, J.J. Eaton-Rye, Specific requirements for cytochrome *c*-550 and the manganese-stabilizing protein in photoautotrophic strains of *Synechocystis* sp. PCC 6803 with mutations in the domain Gly-351 to Thr-436 of the chlorophyll-binding protein CP47, Biochemistry 37 (1998) 14437–14449.
[29] I. Vass, D. Kirilovsky, A.-L. Etienne, UV-B radiation-induced donor- and acceptor-side modifications of Photosystem II in the cyanobacterium *Synechocystis* sp. PCC 6803, Biochemistry 38 (1999) 12786–12794.
[30] J.J. Eaton-Rye, J.A. Shand, W.S. Nicoll, pH-dependent photoautotrophic growth of specific Photosystem II mutants lacking lumenal extrinsic polypeptides in *Synechocystis* PCC 6803, FEBS Lett. 543 (2003) 148–153.
[31] T.C. Summerfield, J.A. Shand, F.K. Bentley, J.J. Eaton-Rye, PsbQ (Sll1638) in *Synechocystis* sp. PCC 6803 is required for Photosystem II activity in specific mutants and in nutrient-limiting conditions, Biochemistry 44 (2005) 805–815.
[32] H. Kless, M. Oren-Shamir, S. Malkin, L. McIntosh, M. Edelman, The *D–E* region of the D1 protein is involved in multiple quinone and herbicide interactions in Photosystem II, Biochemistry 33 (1994) 10501–10507.
[33] P. Mulo, T. Tyystjärvi, E. Tyystjärvi, Govindjee, P. Mäenpää, E.-M. Aro, Mutagenesis of the D–E loop of Photosystem II reaction centre protein D1. Function and assembly of Photosystem II, Plant Mol. Biol. 33 (1997) 1059–1071.
[34] A. Nagarajan, R. Winter, J. Eaton-Rye, R. Burnap, A synthetic DNA fusion PCR approach to the ectopic expression of high levels of the D1 protein of Photosystem II in *Synechocystis* sp. PCC 6803, J. Photochem. Photobiol. B Biol. 104 (2011) 212–219.
[35] R.J. Strasser, A. Srivastava, Govindjee, Polyphasic chlorophyll *a* fluorescence transient in plants and cyanobacteria, Photochem. Photobiol. 61 (1995) 32–42.
[36] R.J. Strasser, M. Tsimilli-Michael, A. Srivastava, Analysis of the chlorophyll *a* fluorescence transient, in: G.C. Papageorgiou, Govindjee (Eds.), Chlorophyll Fluorescence: A Signature of Photosynthesis, Advances in Photosynthesis and Respiration, vol. 19, Springer, Dordrecht, 2004, pp. 321–362.
[37] G.C. Papageorgiou, M. Tsimilli-Michael, K. Stamatakis, The fast and slow kinetics of chlorophyll *a* fluorescence induction in plants, algae and cyanobacteria: a viewpoint, Photosynth. Res. 94 (2007) 275–290.
[38] A. Stirbet, Govindjee, On the relation between the Kautsky effect (chlorophyll *a* fluorescence induction) and Photosystem II: basics and applications of the OJIP fluorescence transient, J. Photochem. Photobiol. B Biol. 104 (2011) 236–257.
[39] J.J.S. Van Rensen, Molecular mechanisms of herbicide action near Photosystem II, Physiol. Plant. 54 (1982) 515–521.
[40] R. Kaňa, E. Kotabová, O. Komárek, B. Šedivá, G.C. Papgeorgiou, Govindjee, O. Prášil, The slow S to M fluorescence rise in cyanobacteria is due to a state 2 to state 1 transition, Biochim. Biophys. Acta 1817 (2012) 1237–1247.
[41] H.H. Robinson, A.R. Crofts, Kinetics of the oxidation reduction reactions of the Photosystem II quinone acceptor complex, and the pathway for deactivation, FEBS Lett. 153 (1983) 221–226.
[42] G. Renger, H.J. Eckert, A. Bergmann, J. Bernarding, B. Liu, A. Napiwotzki, F. Reifarth, H.J. Eichler, Fluorescence and spectroscopic studies of exciton trapping and electron transfer in Photosystem II of higher plants, Aust. J. Plant Physiol. 22 (1995) 167–181.
[43] R.L. Wain, 3:5-Dihalogeno-4-hydroxygenzonitriles as herbicides, Nature 200 (1963) 28.
[44] K. Pfister, K.E. Steinback, G. Gardner, C.J. Arntzen, Photoaffinity labeling of an herbicide receptor protein in chloroplast membranes, Proc. Natl. Acad. Sci. U. S. A. 78 (1981) 981–985.
[45] A. Trebst, W. Draber, Inhibitors of Photosystem II and the topology of the herbicide and Q_B binding polypeptide in the thylakoid membrane, Photosynth. Res. 10 (1986) 381–392.
[46] V. Petrouleas, A.R. Crofts, The iron-quinone complex, in: T.J. Wydrzynski, K. Satoh (Eds.), Photosystem II: The Light-Driven Water: Plastoquinone Oxidoreductase, Advances in Photosynthesis and Respiration, vol. 22, Springer, Dordrecht, 2005, pp. 177–206.
[47] S. Swiatek, R.E. Regel, J. Meurer, G. Wanner, H.B. Pakrasi, I. Ohad, R.G. Herrmann, Effects of selective inactivation of individual genes for low-molecular-mass subunits on the assembly of Photosystem II, as revealed by chloroplast transformation: the *psbEFLJ* operon in *Nicotiana tabacum*, Mol. Gen. Genomics 268 (2003) 699–710.
[48] M. Suorsa, R.E. Regel, V. Paakkarinen, N. Battchikova, R.G. Herrmann, E.-M. Aro, Protein assembly of Photosystem II and accumulation of subcomplexes in the absence of low molecular mass subunits PsbL and PsbJ, Eur. J. Biochem. 271 (2004) 96–107.
[49] P. Mulo, S. Laakso, P. Mäenpää, E.-M. Aro, Stepwise photoinhibition of Photosystem II, Plant Physiol. 117 (1998) 483–490.
[50] T. Takahashi, N. Inoue-Kashino, S. Ozawa, Y. Takahashi, Y. Kashino, K. Satoh, Photosystem II complex *in vivo* is a monomer, J. Biol. Chem. 284 (2009) 15598–15606.
[51] M. Watanabe, M. Iwai, R. Narikawa, M. Ikeuchi, Is the Photosystem II complex a monomer or a dimer? Plant Cell Physiol. 50 (2009) 1674–1680.
[52] P.J. Nixon, F. Michoux, J. Yu, M. Boehm, J. Komenda, Recent advances in understanding the assembly and repair of Photosystem II, Ann. Bot. 106 (2010) 1–16.
[53] Y. Allahverdiyeva, E.-M. Aro, Photosynthetic responses of plants to excess light: mechanisms and conditions for photoinhibition, excess energy dissipation and repair, in: J.J. Eaton-Rye, B.C. Tripathy, T.D. Sharkey (Eds.), Photosynthesis: Plastid Biology, Energy Conversion and Carbon Assimilation, Advances in Photosynthesis and Respiration, vol. 34, Springer, Dordrecht, 2012, pp. 275–297.
[54] A. Mohamed, C. Jansson, Influence of light on accumulation of photosynthesis-specific transcripts in the cyanobacterium *Synechocystis* 6803, Plant Mol. Biol. 13 (1989) 693–700.
[55] Y. Hihara, A. Kamei, M. Kanehisa, A. Kaplan, M. Ikeuchi, DNA microarray analysis of cyanobacterial gene expression during acclimation to high light, Plant Cell 13 (2001) 793–806.
[56] G.-Z. Dai, B.-S. Qiu, K. Forchhammer, Ammonium tolerance in the cyanobacterium *Synechocystis* sp. PCC 6803 and the role of the *psbA* multigene family, Plant Cell Environ. 37 (2014) 840–851.
[57] B. Loll, J. Kern, W. Saenger, A. Zouni, J. Biesiadka, Lipids in Photosystem II: interactions with protein and cofactors, Biochim. Biophys. Acta 1767 (2007) 509–519.
[58] N. Mizusawa, H. Wada, The role of lipids in Photosystem II, Biochim. Biophys. Acta 1817 (2012) 194–208.
[59] M. Hagio, Z. Gombos, Z. Várkonyi, K. Masamoto, N. Sato, M. Tsuzuki, H. Wada, Direct evidence for requirement of phosphatidylglycerol in Photosystem II of photosynthesis, Plant Physiol. 124 (2000) 795–804.
[60] Z. Gombos, Z. Várkonyi, M. Hagio, M. Iwaki, L. Kovács, K. Masamoto, S. Itoh, H. Wada, Phosphatidylglycerol requirement for the function of electron acceptor plastoquinone Q_B in the Photosystem II reaction center, Biochemistry 41 (2002) 3796–3802.
[61] W.L. DeLano, The PyMOL Molecular Graphics System, DeLano Scientific, Palo Alto, 2002.